Electronic Supplementary Information

Strongly coupled carbon nanofiber-metal oxide coaxial nanocables with enhanced lithium storage properties

Genqiang Zhang,[ab] *Hao Bin Wu,*[b] *Harry E. Hoster,*[a] *and Xiong Wen (David) Lou**[ab]

[a] TUM CREATE, 1 CREATE Way, #10-02 CREATE Tower, Singapore 138602

[b] School of Chemical and Biomedical Engineering, Nanyang Technological University, 62 Nanyang Drive, Singapore, 637459

*To whom all correspondence should be addressed. E-mail: xwlou@ntu.edu.sg (X. W. L.); Webpage: http://www.ntu.edu.sg/home/xwlou/

Experimental details

Materials synthesis: The carbon nanofibers (CNFs) are first synthesized through a modified Te-nanowire templating hydrothermal method using glucose as the carbon source.[1,2] The synthesis of CNF@MnO and CNF@$CoMn_2O_4$ coaxial nanocable structures involve a simple two-step process. In a typical synthesis of CNF@MnO nanocables, 3 mmol of $Mn(CH_3COO)_2$ was dissolved into 20 mL of ethylene glycol to form a transparent solution, followed by addition of 60 mg of the as-synthesized CNFs into the solution. After ultrasonication for 30 min to reach well dispersion, the mixture was transferred to a flask and then heated to 170 ^oC in an oil bath. After reaction for 2 h, the solution was cooled down naturally, and then the product of CNF@Mn-glycolate was collected by centrifugation. In order to obtain the CNF@MnO nanocable structure, the CNF@Mn-glycolate was annealed in N_2 at 500 ^oC for 4 h with a heating rate of 3 ^oC min^{-1}. For the synthesis of CFN@$CoMn_2O_4$ nanocables, 1 mmol of $Co(CH_3COO)_2$ and 2 mmol of $Mn(CH_3COO)_3 \cdot 4H_2O$ were used and the annealing temperature was reduced to 420 ^oC to avoid the possible reduction of Mn^{3+} to Mn^{2+} during annealing, while keeping other conditions unchanged. The production for one batch reaction with 20 mL of ethylene glycol is about 0.25 g while it can be easily scaled up to gram-scale with100 mL of ethylene glycol.

Materials Characterization: X-ray diffraction (XRD) patterns were collected on a Bruker D8 Advanced X-Ray Diffractometer. Field-emission scanning electron microscope (FE-SEM) images were obtained on a JEOL JSM 6700F microscope. Transmission electron microscope (TEM) images were taken on a JEOL 2010 microscope. The elemental mapping is performed on energy-dispersive X-ray spectroscopy (EDX) attached to JEOL 2100F microscope. Thermogravimetric analysis (TGA) was carried out under air flow with a temperature ramp of 10 °C min^{-1}.

Electrochemical Measurements: The electrochemical measurements were carried out using CR2016 coin-type half-cells. The working electrode is consisted of active material, carbon black (Super-P-Li), and polymer binder (polyvinylidene fluoride; PVDF) in a weight ratio of 80:10:10. Lithium foil was used as both the counter electrode and the reference electrode. 1M $LiPF_6$ in a 50:50 w/w mixture of ethylene carbonate and diethyl carbonate was used as the electrolyte. Cell assembly was carried out in an Ar-filled glovebox with moisture and oxygen concentrations below 1.0 ppm. The galvanostatic charge-discharge tests were performed on a NEWARE battery test system.

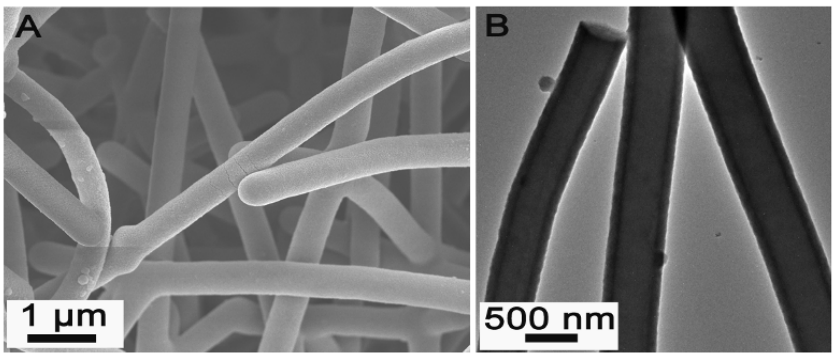

Figure S1. (A) FESEM and (B) TEM images of the CNF@Mn-glycolate coaxial nanocable structure.

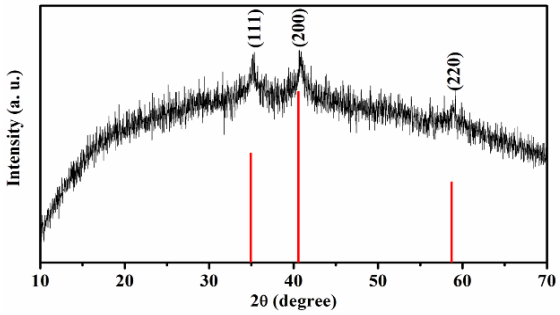

Figure S2. Typical XRD pattern of the CNF@MnO nanocables after annealing at 500 ^{o}C under N_2 for 4 h. All the peaks can be readily indexed to pure MnO phase (JCPDS card No. 78-0424).

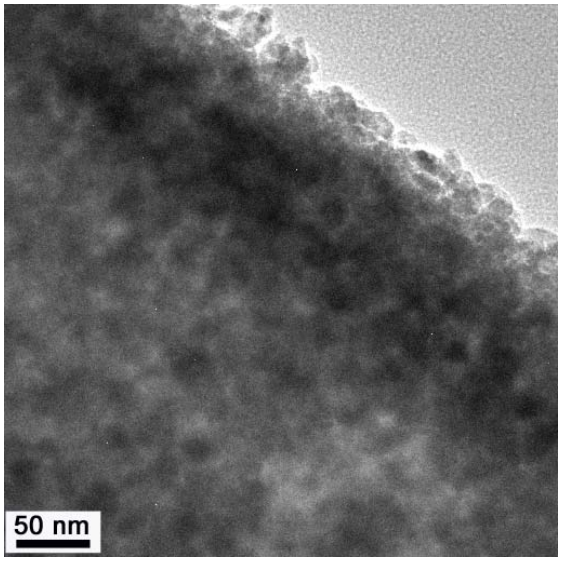

Figure S3. A typical magnified TEM image of the CNF@MnO nanocable.

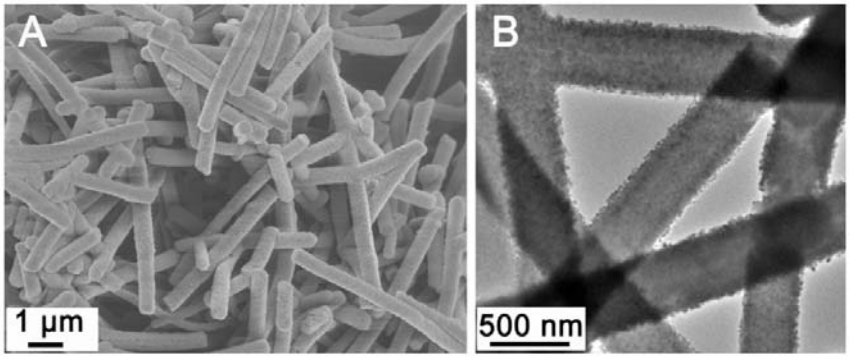

Figure S4. Typical FESEM (A) and TEM (B) images of the CNF@MnO nanocables after sonicating for up to 4 h dispersed in ethanol.

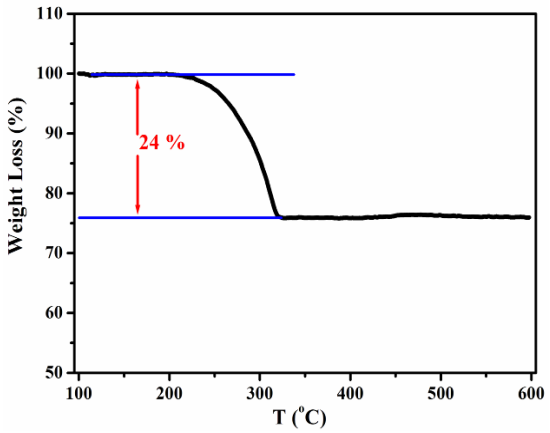

Figure S5. Thermogravimetric analysis (TGA) of the CNF@MnO nanocables in the temperature range of 100 - 600 ^{o}C with a heating rate of 10 ^{o}C min^{-1} in air.

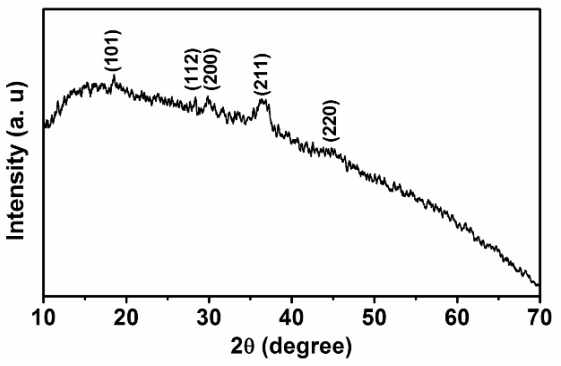

Figure S6. Typical XRD pattern of the CNF@$CoMn_2O_4$ nanocables annealed at 450 ^{o}C in N_2 for 4 h. All the peaks can be readily indexed to pure $CoMn_2O_4$ phase (JCPDS card No. 77-0471).

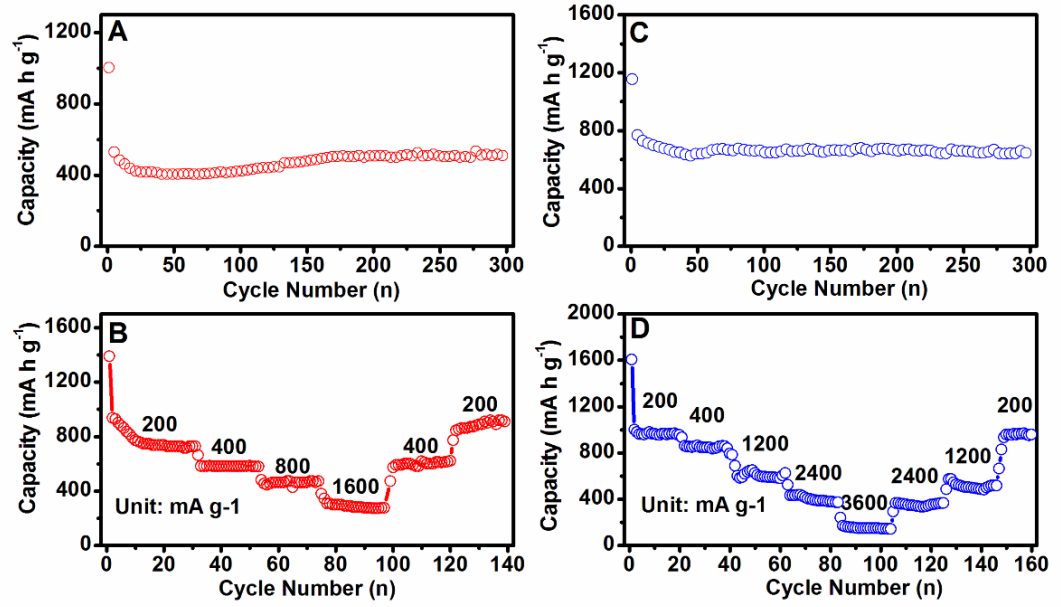

Figure S7. Electrochemical evaluation of CNF@MnO and CNF@$CoMn_2O_4$ coaxial nanocables as anode materials for LIBs: (A, C) Cycling performance at a current density of 1000 mA g^{-1} for CNF@MnO and CNF@$CoMn_2O_4$, respectively. (B, D) Rate capability tested at various current densities from 200 to 3600 mA g^{-1} for CNF@MnO and CNF@$CoMn_2O_4$, respectively.

A brief discussion about the capacity of such hybrid nanocables

In our work, the specific capacity of the CNF@MnO is stabilized at around 750 mA h g^{-1} with a charge/discharge current density of 200 mA g^{-1}. The calculation is based on the total mass of both MnO and CNF in the hybrid nanocable structure, whose percentages are 76 % and 24 %, respectively, determined from the TGA results in Figure S5. The CNF in this work is only annealed at relatively low temperature (500 ^{o}C) under N_2. Therefore, it is reasonable to assume that the CNF will contribute a very low portion to the total capacity. The capacity of the MnO part can then be estimated in the range of 892-955 mA h g^{-1} if we assume the capacity of the CNF is between 100-300 mA h g^{-1} according to the previous literatures[3-6] for un-activated carbon. As we know, the theoretical capacity of the MnO based fully on the conversion mechanism is 698 mA h g^{-1}. Herein, the capacity of the CNF@MnO is much higher than theoretical capacity of MnO. The possible reasons can be described in two aspects: First, it is not uncommon to observe the phenomenon that the specific capacity of nanostructured metal oxides exhibit higher capacity than their theoretical capacities during the previous literatures.[7-12] It is believed that the extra capacity could be ascribed to the reversible formation of organic polymeric/gel like films by decomposition at low potentials, which has also been observed in other MnO/carbon hybrid nanostructures.[7,8] Second, it is proposed that the lithium storage below the electromotive force value is derived from the interfacial charging mechanism, which could also contribute certain amount of the extra capacity. For MnO, the electromotive force is relatively low compared with other transition metal oxides, which is about 1.032 V vs. Li^+/Li.[13,14] Through the charge profiles shown in Figure 4A, the contribution of this part in our work could be estimated as 270 mA h g^{-1}. These two reasons could result in the extra capacity compared with the theoretical capacity and the detailed reasons are still being investigated.

References

1 Liang, H. W.; Guan, Q. F.; Chen, L. F.; Zhu, Z.; Zhang, W. J.; Yu, S. H. *Angew. Chem. Int. Ed.* 2012, **51**, 5101.

2 Zhang, G. Q.; Yu, L.; Hoster, H. E.; Lou, X. W. *Nanoscale* 2013, **5**, 877.

3 Kim, C.; Yang, K. S.; Kojima, M.; Yoshida, K.; Kim, Y. J.; Kim, Y. A.; Endo, M. *Adv. Funct. Mater.* 2006, **16**, 2393.

4 Yoon, S. H.; Park, C. W.; Yang, H. J.; Korai, Y.; Mochida, I.; Baker, R. T. K.; Rodriguez, N. M. *Carbon* 2004, **42**, 21.

5 Doi, T.; Fukuda, A.; Iriyama, Y.; Abe, T.; Ogumi, Z.; Nakagawa, K.; Ando, T. *Electrochem. Commun.* 2005, **7**, 10.

6 Lee, J. K.; An, K. W.; Ju, J. B.; Cho, B. W.; Cho, W. I.; Park, D.; Yun, K. S. *Carbon* 2001, **39**, 1299.

7 Li, X. W.; Xiong, S. L.; Li, J. F.; Liang, X.; Wang, J. Z.; Bai, J.; Qian, Y. T. *Chem. Eur. J.* 2013, **19**, 11310.

8 Sun, Y. M.; Hu, X. L.; Luo, W.; Xia, F. F.; Huang, Y. H. *Adv. Funct. Mater.* 2013, **23**, 2436.

9 Zhang, W. M.; Wu, X. L.; Hu, J. S.; Guo, Y. G.; Wan, L. J. *Adv. Funct. Mater.* 2008, **18**, 3941.

10 Reddy, A. L. M.; Shaijumon, M. M.; Gowda, S. R.; Ajayan, P. M. *Nano Lett.* 2009, **9**, 1002.

11 Cui, L. F.; Yang, Y.; Hsu, C. M.; Cui, Y. *Nano Lett.* 2009, **9**, 3370.

12 Magasinski, A.; Dixon, P.; Hertzberg, B.; Kvit, A.; Ayala, J.; Yushin, G. *Nat. Mater.* 2010, **9**, 353.

13 Yu, X. Q.; He, Y.; Sun, J. P.; Tang, K.; Li, H.; Chen, L. Q.; Huang, X. J. *Electrochem. Commun.* 2009, **11**, 791.

14 Zhong, K.; Zhang, B.; Luo, S.; Wen, W.; Li, H.; Huang, X.; Chen, L. *J. Power Sources* 2011, **196**, 6802.